
MODEL EXPLANATION DISPARITIES AS A FAIRNESS DIAGNOSTIC

Peter W. Chang
SAFR ML Lab
Harvard Business School
pchang@hbs.edu

Leor Fishman
Harvard College
leor.fishman@gmail.com

Seth Neel
SAFR ML Lab
Harvard Business School
sneel@hbs.edu

ABSTRACT

In recent years, there has been a flurry of research focusing on the fairness of machine learning models, and in particular on quantifying and eliminating bias against protected subgroups. One line of work generalizes the notion of protected subgroups beyond simple discrete classes by introducing the notion of a "rich subgroup" [1, 2], and seeks to train models that are calibrated or equalize error rates with respect to these richer subgroup classes. Largely orthogonally, local model explanation methods have been developed that given a classifier h and test point x , attribute influence for the prediction $h(x)$ to the individual features of x . This raises a natural question: *Do local model explanation methods attribute different feature importance values on average across different protected subgroups, and can we detect these disparities efficiently?* If the model places high weight on a given feature in a specific protected subgroup, but not on the dataset overall (or vice versa), this could be a potential indicator of bias in the predictive model or the underlying data generating process, and is at the very least a useful diagnostic that signals the need for a domain expert to delve deeper. In this paper, we formally introduce the notion of feature importance disparity (FID) in the context of rich subgroups, design oracle-efficient algorithms to identify large FID subgroups, and conduct a thorough empirical analysis that establishes auditing for FID as an important method to investigate dataset bias. Our experiments show that across 4 datasets and 4 common feature importance methods our algorithms find (feature, subgroup) pairs that simultaneously: (i) have subgroup feature importance that is often an order of magnitude different than the importance on the dataset as a whole (ii) generalize out of sample, and (iii) yield interesting discussions about potential bias inherent in these datasets.

1 Introduction

Machine learning is rapidly becoming both a more important and more opaque part of our day to day lives and decision making – with increasingly high stakes use cases such as recidivism analysis [3], loan granting and terms [4] and child protective services [5]. One of the hopes with this deployment of wide-scale ML has been that those algorithms might be somehow free of our human biases and imperfections. It turns out that this hope was, unfortunately, naive. Over the last decade, an interdisciplinary body of research has shown that machine learning algorithms can be deeply biased in both subtle and direct ways [6], and has focused on developing countless techniques to produce fairer models [7]. One of the primary causes of model bias is bias that is inherent in the training data, rather than an explicitly biased training procedure. The issue of biased training data causing bias in downstream model predictions is particularly concerning in light of modern machine learning, where an initial "foundation model" like GPT-3 [8] or CLIP [9] is trained on a very large corpus of text or image data and released publicly, which an algorithm designer then fine tunes using a much smaller dataset tailored for a specific use case. Social biases present in the training data of the foundation model then have the potential to propagate into the myriad use cases built on top of it [10, 11]. While the threat posed by these

foundation models is new, the recognition that bias in the training data could propagate into unfair decisions made by a classifier is not; in a 2015 in a New York Times interview [12], Cynthia Dwork, widely regarded as pioneer in the field of algorithmic bias, describes the problem as such:

Suppose we have a minority group in which bright students are steered toward studying math, and suppose that in the majority group bright students are steered instead toward finance. An easy way to find good students is to look for students studying finance, and if the minority is small, this simple classification scheme could find most of the bright students. But not only is it unfair to the bright students in the minority group, it is also low utility. Now, for the purposes of finding bright students, cultural awareness tells us that “minority+math” is similar to “majority+finance.” A classification algorithm that has this sort of cultural awareness is both more fair and more useful.

Unpacking this example, we see that the fundamental issue is that a classifier trained on the entire population would learn the rule that students who study finance are bright, whereas in the minority population bright students actually study mathematics, and so this rule would systematically disadvantage them. Put a different way, the feature `is-math-major` is highly predictive in the minority group but not at all in the majority group, while `is-finance-major` is predictive in the population at large but not in the minority group. While in this simple example it is clear that it is the differing impact of these features that causes the downstream classifier to become biased, in many practical machine learning settings the situation is far more complex. As models grow in complexity and input datasets grow in dimension, understanding how a specific feature contributes to a model’s prediction becomes an increasingly difficult task, and is the focus of research into feature importance methods. These methods seek to attribute credit for a given prediction $\hat{y} = \theta(x_{test})$ across features present in x_{test} . For inherently interpretable models like linear regressions this is clear, because the contribution of feature i is captured by the i^{th} regression coefficient, but for more complex models like neural networks or random forests, there is no natural notion of feature importance. New techniques designed to address these more practical settings have garnered substantial attention, and include local model agnostic methods like LIME [13], SHAP [14], model-specific saliency maps [15], and example-based counterfactual explanations [16] which we discuss more in Section 1.2. These new methods raise an obvious question in light of the prior discussion, although one that to the best of our knowledge has not been thoroughly studied:

When applied to real classifiers and datasets where bias is a key concern, do these popular feature importance methods uncover substantial differences in feature importance across protected groups?

It is known that while a classifier may look fair when comparing a given fairness metric across a handful of sensitive subgroups, when the notion of a sensitive subgroup is generalized to encompass combinations and interactions between sensitive features (known as *rich subgroups* [17]), large disparities can emerge. Since even for simple notions of a rich subgroup such as conjunctions of binary features there are exponentially many, how to efficiently search among the subgroups for the ones with large disparities in fairness metrics is not immediately obvious, an issue addressed by the well-known oracle-efficient algorithms in [1, 2]. In this paper, we formally introduce the notion of *feature importance disparity* (FID) in the context of rich subgroups, design oracle-efficient algorithms to identify large FID subgroups, and conduct a thorough empirical analysis that establishes auditing for FID as an important method to investigate dataset bias across a range of feature importance methods, classifiers, and datasets. Importantly, we eschew any broader claims that large FID values necessarily imply a mathematical conclusion about the *fairness* of the underlying classification model in all cases, and we suspect that pursuing such a direction would likely be a fool’s errand. It is known that even the most popular and natural fairness metrics are impossible to satisfy simultaneously, and so we would run up against the problem of determining what it means for a model to be *fair* [18, 19]. Moreover, it is known that the most widely used feature importance methods, including the ones we study, are often at odds with each other, and so none can be considered definitive [20]. Rather we take the perspective that rooting out dataset bias must be a collaborative process involving a domain expert, and should involve an interrogation of what features are present in the dataset, and how they may have been collected, measured, or interpreted differently, for different subgroups. The methods developed here represent a part of the algorithmic toolkit we hope can aid the data analyst or domain expert in this multi-faceted process. We now elaborate further on our contributions.

1.1 Results

Our most important contribution is formalizing the notion of *feature importance disparity* (FID and its related variants), in the context of new feature importance methods developed in recent years, and with respect to rich subgroups (Definition 1). We categorize the feature importance method for a subgroup as *separable* or not, based on whether it can be expressed as a sum over points in the subgroup (Definition 2). Our main theoretical contribution is Theorem 1 in Section 3, which says informally that although the problem of finding the maximal FID subgroup is NP-hard in the worst case (Appendix C), given access to an oracle for *cost-sensitive classification* with respect to the rich subgroup class

\mathcal{G} , (Definition 5), Algorithm 1 efficiently learns the subgroup with maximal FID for any separable feature importance method.

Algorithm 1 is inspired by prior work [1, 21, 2] that takes a constrained optimization and solves the equivalent problem of computing the Nash equilibrium of a two-player zero-sum game given by the Lagrangian. In Algorithm 1 we compute the equilibrium of the game by having both the min and max players implement *no-regret* strategies – something we show can be done efficiently given access to a CSC oracle for \mathcal{G} . This CSC oracle is implemented via simple regression heuristic (Algorithm 2 in the Appendix) which our experimental results show works well in practice. In Section 4, we introduce a non-separable notion of subgroup feature importance based on linear regression, and develop a heuristic approach to find large FID subgroups and to control the size of these subgroups via a regularization term. This approach finds the largest FID subgroup by optimizing a non-convex differentiable expression for the FID with ADAM [22].

In Section 5, we conduct a thorough empirical evaluation of our methods, auditing for large FID subgroups on the Student [23], COMPAS [3], Bank [24], and Folktables [25] datasets, using LIME [13], SHAP [14], GRAD [15], and linear regression coefficient [16] as our feature importance methods. Our experiments establish that:

- Across all (dataset, feature importance method) pairs, we are able to find subgroups defined as simple functions of the sensitive features that have large AVG-FID with respect to a specific feature (Table 2, Figures 1, 2)!
- Inspecting the coefficients that define the sensitive subgroups, we are able to pull out interesting examples where a subgroup, largely defined by a few sensitive features like race and gender, has a large FID with respect to a given feature, highlighting potential bias in the data and warranting a closer investigation (Subsection 5.3, Figure 3).
- A natural question to ask is if focusing on AVG-FID on rich subgroups is overkill; perhaps similar levels of disparities exist when we restrict our attention to simpler subgroup classes that are a function of a single sensitive attribute (marginal subgroups). In Subsection 5.5, we compare the maximal AVG-FID found for a rich subgroup, to the AVG-FID found when we restrict our subgroup class to marginal subgroups. We find that in about half of the settings the rich subgroup achieves a higher AVG-FID out of sample, justifying the use of rich subgroups. We note that examining FID even in the context of marginal subgroups has not been done in prior work.
- We show that our FID’s generalize out of sample and that our method for controlling subgroup size is effective. (Figures 4a, 4b, 5)

Taken together, our theoretical and empirical results highlight our methods as an important addition to the toolkit for detecting bias in tabular datasets with sensitive features.

1.2 Related Work

There is a substantial body of work investigating issues of bias in the context of machine learning, including notions of rich subgroups or multicalibration, and on techniques for assigning feature importance with respect to a classifier’s predictions. To the best of our knowledge this is the first work investigating the disparity in feature importance measures when computed on rich subgroups.

Rich Subgroups and Multicalibration. At a technical level, the most closely related papers are [1, 2] which introduce the notion of the rich subgroup class \mathcal{G} over sensitive features in the context of learning classifiers that are with respect to equalized odds or calibration. Our Algorithm 1 fits into the paradigm of “oracle-efficient” algorithms for solving constrained optimization problems introduced in [21] and developed in the context of rich subgroups in [1, 17, 2]. There has been much recent interest in learning multicalibrated predictors because of connections to uncertainty estimation and omnipredictors [26, 27, 28]. None of these works consider feature importance disparities.

Fairness in Machine Learning. More generally, the idea that machine learning systems can replicate or amplify the bias inherent in their training data has been studied in thousands of papers in recent years – [6, 7] are definitive references for developments in the field. These papers typically concern the implementation of a new fairness notion in a given learning setting; either an individual fairness notion [29, 30], one based on equalizing a statistical rate across protected subgroups [31, 32], or one based on an underlying causal model [33]. With a given notion of fairness in hand, approaches to learning fair classifiers can be typically classified as “in-processing”, or trying to simultaneously learn a classifier and satisfy a fairness constraint, “post-processing” which takes a learned classifier and post-processes it to satisfy a fairness definition [31], or most closely related to the motivation behind this paper, pre-processing the data to remove bias. Although none of these works consider feature importance as a fairness diagnostic, we are motivated at a high level by existing work on dataset bias [34, 35, 36].

Feature Importance Methods. The field of interpretable or explainable machine learning attempts to explain *why* a model h makes a specific prediction $h(x) = y$. We refer the reader to [16] for a survey of methods. The most relevant work to this paper are those methods that can be leveraged to investigate the importance of a feature f_j in a given subset of the dataset S . Local interpretation methods assign a feature importance f_j for every point (x, y) , and so they can be used to define a notion of importance in a subgroup by summing or average over the points in the subgroup as we do in Definitions 2, 3. These methods include model-agnostic methods like LIME or SHAP [13, 14], methods like saliency maps [15, 37, 38] that require h to be differentiable in x , or model-specific methods that depend on the classifier. Global methods attempt to explain the entire model behavior, and so can be run on the entire subgroup; our LIN-FID is a global method that relies on training an inherently interpretable model (linear regression) on the subgroup and inspecting its coefficients. Other inherently interpretable models that could be used to define a notion of subgroup importance include decision trees [39] and generalized additive models [40].

Fairness and Interpretability. Although no existing work examines the role of feature importance methods in detecting disparities in rich subgroups, there is a small amount of existing work examining explainability in the context of fairness. The recent [41] formalizes induced discrimination as a function of the SHAP values assigned to sensitive features, and proposes a method to learn classifiers where the protected attributes have low influence. [42] applies a similar approach, attributing a models overall unfairness to its individual features using the Shapley value, and proposing an intervention to improve fairness. [43] examines machine learning models to predict recidivism, and empirically shows tradeoffs between model accuracy, fairness, and interpretability.

2 Preliminaries

Let X^n represent our dataset, consisting of n individuals defined by the tuple $((x, x'), y)$ where $x \in \mathcal{X}_{sense}$ is the vector of protected features, $x' \in \mathcal{X}_{safe}$ is the vector of unprotected features, and $y \in \mathcal{Y}$ denotes the label. With $X = (x, x') \in \mathcal{X} = \mathcal{X}_{sense} \times \mathcal{X}_{safe} \subset \mathbb{R}^d$ denoting a joint feature, the data points (X, y) are drawn i.i.d from a distribution \mathcal{R} . Let $h : \mathcal{X} \rightarrow \mathcal{Y}$ denote a classifier or regressor that predicts y from X . We define a *rich subgroup class* $\mathcal{G} = \{g_\alpha\}_{\alpha \in \Omega}$ as a collection of functions $g : \mathcal{X}_{sens} \rightarrow [0, 1]$, where $g(x')$ denotes the membership of point $X = (x, x')$ in group g . Note that this is the same definition of subgroup as in [1], but without the constraint that $g(x') \in \{0, 1\}$, which supports varying degrees of group membership. For example, a biracial person may be .5 a member of one racial group and .5 a member of another. Let $f_j, j \in [d]$ denote the j^{th} feature in $\mathcal{X} \subset \mathbb{R}^d$. Then for a classifier h and subgroup $g \in \mathcal{G}$, let $F(f_j, g, h)$ denote the *importance h attributes to feature j in the subgroup g* , and $F(f_j, X^n, h)$ be the importance h attributes to f_j on the entire dataset. We will provide specific instantiations of $F(\cdot)$ shortly, but we state our definition of FID in the greatest possible generality below.

Definition 1. (*Feature Importance Disparity*). Given a classifier h , a subgroup defined by $g \in \mathcal{G}$, and a feature $f_j \in [d]$. Then given a feature subgroup importance measure $F(\cdot)$, the feature importance disparity relative to g is defined as:

$$FID(f_j, g, h) = \mathbb{E}_{X \sim \mathcal{R}} |F(f_j, X^n, h) - F(f_j, g, h)|$$

We will suppress h and write $FID(g, j)$ unless it is necessary to clarify what classifier we are describing. Now given h and X^n , in this paper we will investigate the problem of finding the feature subgroup pair $(j^*, g^*) \in [d] \times \mathcal{G}$ that maximizes $FID(j, g)$, or $(j^*, g^*) = \operatorname{argmax}_{g \in \mathcal{G}, j \in [d]} FID(g, j)$. Since we may not be interested in extremely small or large groups, we will also impose the constraint that the group size $|g| = \frac{1}{n} \sum_{X \in X^n} g(X)$ is between $[\alpha_L, \alpha_U]$, defining

$$(j^*, g^*)_{\alpha_L, \alpha_U} = \operatorname{argmax}_{g \in \mathcal{G}, |g| \in [\alpha_L, \alpha_U], j \in [d]} FID(g, j)$$

Without constraining the group size, in the case when $F'(f_j, x, h) > 0 \forall x$, Definition 1 is maximized when $|g| \approx 0$. Although the local feature importance methods F' don't force $F'(f_j, x, h) > 0$, on datasets where the features typically had positive importance values, solving the CSC problem would return a subgroup with size close to 0. On these datasets, it is important to be able to impose bounds on the subgroup size to avoid this degenerate case. We now get more concrete about our subgroup feature importance measure $F(f_j, g, h)$. In this paper we study two classes of importance measure, those that are *separable* and *non-separable*. We define a *separable* feature importance measure as one that can be decomposed as a point wise sum of feature importances.

Definition 2. (*Locally Separable FID*). Given a local model explanation [16] that attributes a proportion of the prediction of h on $x \in X$ to feature j , denoted by $F'(f_j, x, h)$, we define the corresponding

$$FID(f_j, g, h) = \mathbb{E}_{X^n \sim \mathcal{R}^n} \left| \sum_{X \in X^n} g(X) F'(f_j, X, h) - \sum_{X \in X^n} F'(f_j, X, h) \right|$$

Given a local model explanation F' , we can also define the AVG-FID, which compares the average feature importance within a subgroup to the average importance on the dataset.

Definition 3. (*Average Case Locally Separable FID*). For $g \in \mathcal{G}$, let $|g| = \sum_{X \in X^n} g(X)$. Given a local model explanation $F'(f_j, X, h)$, we define the corresponding

$$\text{AVG-FID}(f_j, g, h) = \mathbb{E}_{X^n \sim \mathcal{R}^n} \left| \frac{1}{|g|} \sum_{X \in X^n} g(X) F'(f_j, X, h) - \frac{1}{n} \sum_{X \in X^n} F'(f_j, X, h) \right|$$

Note that AVG-FID is not equivalent to a separable FID, since we are dividing by $\frac{1}{|g|}$ which impacts every term in the summation. Popular local model explanations that we use to define FID or AVG-FID notions include LIME [13], Shapley Additive Explanations [14], and gradient-based saliency maps [15]. The non-separable FID notion considered in this paper corresponds to training a model that is inherently interpretable on only the data in the subgroup g , and comparing the influence of feature j to the influence when trained on the dataset as a whole. Since all of the points in the subgroup can interact to produce the interpretable model, this notions typically won't be separable. Below we formalize this in the case of linear regression, which is the non-separable notion we investigate in the experiments.

Definition 4. (*Linear Feature Importance Disparity*). Given a subgroup g , let $\theta_g = \inf_{\theta \in \mathbb{R}^d} \mathbb{E}_{(X,y) \sim \mathcal{R}} [g(X)(\theta'X - y)^2]$, and $\theta_{\mathcal{R}} = \inf_{\theta \in \mathbb{R}^d} \mathbb{E}_{(X,y) \sim \mathcal{R}} [(\theta'X - y)^2]$. Then if e_j is the j^{th} basis vector in \mathbb{R}^d , we define the linear feature importance disparity (*LIN-FID*) by

$$\text{LIN-FID}(g, j) = |(\theta_g - \theta_{\mathcal{R}}) \cdot e_j|$$

$\text{LIN-FID}(g, j)$ is defined as the difference between the coefficient for feature j when training the model on the subgroup g , versus training the model on points from \mathcal{R} . While this is an appealing notion due to it's simplicity, it is not relevant in the setting where the design matrix in the subgroup is not full rank. In practice we overcome this issue when finding the largest LIN-FID subgroup by lower bounding the size of the subgroups g by adding a regularization term, and by adding a very small l_2 norm penalty to the optimization to force the matrix to be full rank. We discuss these details further in Section 5. We also note that LIN-FID is a similar notion to that of LIME [13], but LIME estimates a local effect around each point which is then summed to get the effect in the subgroup, and so it is *separable*.

This notion of *separability* is crucial to understanding the remainder of the paper. In Section 3, we show that for any *separable* FID, Algorithm 1 is an (oracle) efficient way to compute the largest FID subgroup of a specified size in polynomial time. By "oracle efficient" we follow the paradigm of [21, 1] where we mean access to a type of optimization oracle that can solve (possibly NP-hard) problems. While this sounds like a strong assumption, in practice we can take advantage of state-of-the-art optimization algorithms that are able to solve hard non-convex optimization problems in practice (for example training neural networks). This framework has led to the development of practical algorithms with a strong theoretical grounding in many recent works [21, 1, 17, 2], and as shown in Section 5 works well in practice here as well.

The type of optimization oracle we need is called a Cost Sensitive Classification (CSC) oracle, which we now define.

Definition 5. (*Cost Sensitive Classification*) A *Cost Sensitive Classification problem (CSC)* for a hypothesis class \mathcal{G} is given by a set of n tuples $\{(X_i, c_i^0, c_i^1)\}_{i=1}^n$, where c_i^0 and c_i^1 are the costs of assigning labels 0 and 1 to X_i respectively. A CSC oracle finds the classifier $\hat{g} \in \mathcal{G}$ that minimizes the total cost across all points:

$$\hat{g} = \operatorname{argmin}_{g \in \mathcal{G}} \sum_i \left(g(X_i) c_i^1 + (1 - g(X_i)) c_i^0 \right) \quad (1)$$

3 Locally Separable FID

In this section, we present Algorithm 1, which shows that for any separable FID and rich subgroup class \mathcal{G} , given access to a CSC oracle for \mathcal{G} , we can efficiently compute the subgroup g that maximizes the FID subject to group size constraints. We focus on optimizing the constrained FID since this primitive also allows us to efficiently optimize AVG-FID:

1. Discretize $[0, 1]$ into intervals $(\frac{i-1}{n}, \frac{i}{n}]_{i=1}^n$, and for a given feature f_j compute $g_{(\frac{i-1}{n}, \frac{i}{n}]}$ for $i = 1 \dots n$
2. Outputting g_{k^*} , where $k^* = \operatorname{argmax}_k \frac{k}{n} |F(f_j, g_k, h)|$ approximately maximizes the AVG-FID.

Thus whether we are solving the unconstrained or average-case FID problem, it is sufficient to be able to solve the constrained FID problem:

$$\begin{aligned}
 & \max_{g \in \mathcal{G}} |F(f_j, g(X), h) - F(f_j, X, h)| \\
 & \text{s.t. } \Phi_L(g) \equiv \alpha_L - \sum_{x \in X} g(x) \leq 0 \\
 & \Phi_U(g) \equiv \sum_{x \in X} g(x) - \alpha_U \leq 0
 \end{aligned} \tag{2}$$

Where Φ_L and Φ_U are "size violation" functions given a subgroup function g .

We start by showing that for the unconstrained problem computing the subgroup g_j^* that maximizes $\text{FID}(f_j, g, h)$ over \mathcal{G} can be computed in two calls to $\text{CSC}_{\mathcal{G}}$ when FID is separable.

Lemma 1. *If F is separable and $\text{CSC}_{\mathcal{G}}$ is a CSC oracle for \mathcal{G} , then for any feature f_j , g_j^* can be computed with two oracle calls.*

Proof. By definition $g_j^* = \text{argmax}_{g \in \mathcal{G}} \text{FID}(g, j) = \text{argmax}_{g \in \mathcal{G}} |F(f_j, X^n, h) - F(f_j, g, h)| = \text{argmax}_{g \in \{g^+, g^-\}} \text{FID}(g, j)$, where $g^+ = \text{argmax}_{g \in \mathcal{G}} F(f_j, g, h)$, $g^- = \text{argmin}_{g \in \mathcal{G}} F(f_j, g, h)$. By the definition of separability, we can write

$$F(f_j, g(X), h) = \sum_{x \in g(X)} F'(f_j, x, h) = \sum_{i=1}^n g(x_i) F'(f_j, x_i, h)$$

Then letting $c_k^0 = 0$ for $k = 1, \dots, n$, $c_k^1 = -F'(f_j, x_i, h)$, we see that $g^+ = \text{CSC}_g((c_k^0, c_k^1))$, $g^- = \text{CSC}_g((c_k^0, -c_k^1))$. This establishes the claim. \square

We now state our main theorem, which shows that we can solve the constrained FID problem in Equation 2 with polynomially many calls to $\text{CSC}_{\mathcal{G}}$.

Theorem 1. *Let F be a separable FID notion, fix a classifier h , subgroup class \mathcal{G} , and oracle $\text{CSC}_{\mathcal{G}}$. Then fixing a feature of interest f_j , we will run Algorithm 1 twice; once with FID given by F , and once with FID given by $-F$. Let $\hat{p}_{\mathcal{G}}^T$ be the distribution returned after $T = O(\frac{4n^2 B^2}{\nu^2})$ iterations by Algorithm 1 that achieves the larger value of $\mathbb{E}[\text{FID}(g, j)]$. Then:*

$$\begin{aligned}
 & \text{FID}(g_j^*, j) - \mathbb{E}_{g \sim \hat{p}_{\mathcal{G}}^T} [\text{FID}(g, j)] \leq \nu \\
 & |\Phi_L(g)|, |\Phi_U(g)| \leq \frac{1 + 2\nu}{B}
 \end{aligned} \tag{3}$$

We defer the proof of Theorem 1 to Appendix A, which proceeds as follows:

- Since $F(f_j, X^n, h)$ doesn't depend on g , to optimize Equation 2, we can replace the objective with $F(f_j, g(X), h)$ and $-F(f_j, g(X), h)$, solving two constrained optimizations, and choosing the subgroup g with the largest value of $|F(f_j, g(X), h) - F(f_j, X^n, h)|$.
- Rather than optimizing over $g \in \mathcal{G}$, we optimize over distributions $\Delta(\mathcal{G})$. This allows us to cast the optimization problem in Equation 2 as a linear program.
- By strong duality for finite LPs, we can solve the LP as a min-max problem, where we minimize FID, and maximize the subgroup size violations over the dual variables.
- We can apply Sion's minimax Theorem [44] to cast this as computing the Nash equilibrium of a two-player zero-sum game, and then apply the classical result of [45] which says that if both players implement *no-regret* strategies, then we converge to the Nash equilibrium at a rate given by the average regret of both players converging to zero.
- Algorithm 1 implements the no-regret algorithm exponentiated gradient descent [46] for the max player, and best-response for the min player.
- Since the best-response for the min player can be compute with a single call to $\text{CSC}_{\mathcal{G}}$ (Line 9 of Algorithm 1), Algorithm 1 is oracle-efficient, making 1 oracle call per round t .

Algorithm 1 Iterative Constrained Optimization

1: **Input:** Dataset X^n , $|X^n| = n$, hypothesis h , feature of interest f_j , feature importance function F , size constraints α_L and α_U , size violation indicators Φ_U and Φ_L , and CSC oracle for \mathcal{G} , $CSC_{\mathcal{G}}(c^0, c^1)$, bound B , tolerance ν .

2: **Initialize:**

3: Feature importance vector $\mathbf{C} = (F(f_j, X_i, h))_{i=1}^n$

4: Set $\theta_1 = (0, 0)$

5: $\eta = \frac{\nu}{2n^2 B}$

6: **for** $t = 1, 2, \dots$ **do**

7: $\lambda_{t,0} = B \frac{\exp(\theta_{t,0})}{1 + \exp(\theta_{t,0})}$, $\lambda_{t,1} = B \frac{\exp(\theta_{t,1})}{1 + \exp(\theta_{t,1})}$

8: $c_t^1 = (\mathbf{C}_i - \lambda_{t,0} + \lambda_{t,1})_{i=1}^n$

9: $g_t = CSC_{\mathcal{G}}(\mathbf{0}, c_t^1)$

10: $\hat{p}_{\mathcal{G}}^t = \frac{1}{t} \sum_{t'=1}^t g_{t'}$, $\lambda'_t = (B\Phi_L(\hat{p}_{\mathcal{G}}^t), B\Phi_U(\hat{p}_{\mathcal{G}}^t))$, $\bar{L} = L(\hat{p}_{\mathcal{G}}^t, \lambda'_t)$

11: $\hat{p}_{\lambda}^t = \frac{1}{t} \sum_{t'=1}^t (\lambda_{t',0}, \lambda_{t',1})$, $g'_t = CSC_{\mathcal{G}}(\mathbf{0}, (\mathbf{C}_i - \hat{p}_{\lambda_0}^t + \hat{p}_{\lambda_1}^t)_{i=1}^n)$, $\underline{L} = L(g'_t, \hat{p}_{\lambda}^t)$

12: $v_t = \max(|L(\hat{p}_{\mathcal{G}}^t, \hat{p}_{\lambda}^t) - \underline{L}|, |\bar{L} - L(\hat{p}_{\mathcal{G}}^t, \hat{p}_{\lambda}^t)|)$

13: **if** $v_t \leq \nu$ **then**

14: Return $\hat{p}_{\mathcal{G}}^t, \hat{p}_{\lambda}^t$

15: **end if**

16: Set $\theta_{t+1} = \theta_t + \eta(\alpha_L - |g_t|, |g_t| - \alpha_U)$

17: **end for**

We note that rather than computing the group g that maximizes $\text{FID}(g, j)$ subject to the size constraint, our algorithm outputs a distribution over groups $\hat{p}_{\mathcal{G}}^T$ that satisfies this process *on average* over the groups. In theory this seems like a drawback since our goal is to find sensitive subgroups with a clean interpretation in terms of the sensitive features, and with a large FID. However, in practice we simply take the groups g_t found at each round and output the ones that are in the appropriate size range, and have largest FID values. The results in Section 5 validate that this heuristic choice is able to find groups that are both feasible, and have very large FID values that generalize out of sample. Moreover, the feature that our method provides a menu of potential groups $(g_t)_{t=1}^T$ that can be quickly evaluated for large FID is a useful one as we may uncover interesting biases that aren't present in the maximal subgroup.

4 Approach: Non-Locally Separable Importance Notions

In this section, we discuss the non-locally separable notion of feature importance based on linear regression we introduced in the preliminaries, LIN-FID. Since Algorithm 1 relies crucially on F being separable, we have to use a different heuristic approach to computing the subgroup with largest AVG-FID.

4.1 Linear Regression Coefficients as an Importance Notion

Expanding Definition 4 using the standard weighted least squares estimator (WLS), the feature importance for a given feature f_j and subgroup $g(X)$ is:

$$F_{lin}(g, j) = ((Xg(X)X^T)^{-1}(X^Tg(X)Y)) \cdot e_j, \quad (4)$$

Where $g(X)$ is a diagonal matrix of the output of the subgroup function. The coefficients of the linear regression model on the dataset X can be computed using the results from ordinary least squares (OLS): $(XX^T)^{-1}(X^TY) \cdot e_j$.

We compute $\text{argmax}_{g \in \mathcal{G}} \text{LIN-FID} = \text{argmax}_{g \in \mathcal{G}} |F_{lin}(X^n, j) - F_{lin}(g, j)|$ by finding the minimum and maximum values of $F_{lin}(g, j)$. For the experiments in Section 5, we use logistic regression as the hypothesis class for g because it is non-linear enough to capture complex relationships in the data, but maintains interpretability in the form of its coefficients, and importantly because Equation 4 is then differentiable in the parameters θ of $g(X) = \sigma(X \cdot \theta)$, $\sigma(x) = \frac{1}{1 + e^{-x}}$. Since Equation 4 is differentiable in θ , we can use non-convex optimizers like SGD or ADAM to maximize Equation 4 over θ . It can be shown that F_{lin} is nonconvex (see Appendix B) which means the stationary point we converge to via gradient descent may only be locally optimal. As noted in the preliminaries, in practice we need to ensure the matrix $Xg(X)X^T$ is of full rank. We do this first by lower bounding the size of g via a size penalty term $P_{size} = \max(\alpha_L - |g(X_{train})|, 0) + \max(|g(X_{train})| - \alpha_U, 0)$, which allows us to provide α constraints in the same manner as in the separable approach. We also add a small l_2 regularization term ϵI to $X^Tg(X)X$. This forces the

matrix to be invertible, avoiding issues with extremely small subgroups. Incorporating these regularizers, Equation 4 becomes:

$$F_{lin}(g, j) = \lambda_s \cdot ((X\sigma(X \cdot \theta_L^T)X^T + \epsilon I)^{-1}(X^T \sigma(X \cdot \theta_L^T)Y) \cdot e_j) + \lambda_c \cdot P_{size} \quad (5)$$

In Section 5, we optimize Equation 5 using the ADAM optimizer [22].

5 Experiments

In Subsection 5.1, we discuss the datasets used, FID notions studied, and algorithmic details. In Subsection 5.2 we report the results of our extensive empirical investigation, showing that across 16 different dataset/FID-notion pairings our methods return interesting subgroups defined as a function of sensitive features that exhibit order of magnitude AVG-FID values that are valid out of sample. In Subsection 5.5, we compare AVG-FID values found over rich subgroups, to the AVG-FID value found over marginal subgroups. Specifically we show the following:

- Our approach works in finding subgroups with high AVG-FID subgroups defined by sensitive characteristics, across all datasets and FID notions studied (Figure 1, 3).
- These subgroup/feature pairs raise interesting questions about feature importance disparities in some of the most common datasets used in the fairness and interpretability literatures (Figure 3, Subsection 5.3).
- Examining the distribution of AVG-FID values across the maximal subgroup we find for each feature, we see that they are large for a few features but tail off for the majority of features (Figure 2).
- Our Algorithm 1 to solve the constrained FID consistently produce appropriately sized subgroups with subgroup sizes and FID values that generalize to the test set, across all separable FID notions studied and different hypothesis classes h (Figures 4, 5). Our algorithms converge to a (locally) optimal subgroup g that maximizes the constrained FID (Appendix G, H).
- Figure 6 shows that in half of the settings studied, AVG-FID over the rich subgroup class is higher than over the marginal subgroup class, with some dataset method pairs ((Student, SHAP), (Folktables, LR)) witnessing particularly large gaps.

5.1 Experimental Details

Datasets. We used four datasets for the experiments: Student[23], COMPAS [3], Bank [24], and Folktables [25]. The datasets cover a diverse range of applications: prediction of student performance using familial and demographic data in a Portuguese school, prediction of recidivism or decile risk score using a pre-trial defendant’s personal background and past criminal background, prediction of whether a potential client signed up for a bank account using features including age and marital status, and a dataset derived from US Census Data that uses demographic data from the state of Michigan to predict whether a person’s income exceeds 50K. The datasets were selected on the basis of three criteria: (i) they all use features, some of which could be considered *sensitive* to make predictions about individuals in a context where bias is a significant concern (ii) they are heavily used datasets in research on interpretability and fairness, and as such issues of bias in the datasets should be of importance to the community, and (iii) they trace out a range of number of datapoints and number of features and sensitive features, which we summarise in Table 1. For each dataset, we specified features that were "sensitive." That is, when searching for subgroups with high FID, we only considered rich subgroups defined by features generally covered by equal protection or privacy laws (e.g. race, gender, age, health data). We discuss this further in Appendix D.

Computing the AVG-FID. We study 4 notions of FID – 3 separable notions based on local model explanations Local-Interpretable, Model-Agnostic (LIME) [13], Shapley Additive Explanations (SHAP) [14], the vanilla gradient approach we call GRAD [15] – and the nonseparable LIN-FID (Definition 4). For details on how we implemented these notions including software packages used, see Appendix D. For every method and dataset, we optimize the constrained FID over α ranges $(\alpha_L, \alpha_U) = \{ [.01, .05], [.05, .1], [.1, .15], [.15, .2], [.2, .25] \}$. These small ranges allowed us to reasonably compare the AVG-FID, which is reported in Table 2. Additionally, these ranges spanning 1% to 25% of the total dataset represent subgroup sizes that may be of particular interest in fairness research and dataset auditing work. All values of AVG-FID reported in Table 2 and Figures 1, 3 are *out of sample*; e.g. the AVG-FID values are computed on a test set that was not used to optimize the subgroups. For the separable approach, all datasets were split into a train and test set each containing half of the data. Across all datasets, when the FID was LIME or SHAP we set h to be a random forest, when it was GRAD we used logistic regression as we require a classifier whose outputs are differentiable in the inputs, and for LIN-FID we are implicitly using linear regression. The random forest hyperparameters were set to the default sci-kit learn values with a random seed of 0.

Table 1: Summary of Datasets

Dataset	Data Points	# of Features	# of Sensitive Features
Student	395	32	6
COMPAS	6172	95	8
Bank	30488	57	4
Folktables Income	50008	52	16

Table 2: Summary of highest FIDs found for each experiment along with corresponding feature, subgroup size, and defining features, defined as the two sensitive features with the largest coefficients in g . Experiments were run across ranges $(\alpha_L, \alpha_U) = \{[.01, .05], [.05, .1], [.1, .15], [.15, .2], [.2, .25]\}$ with only the highest AVG-FID found being displayed.

Dataset	Notion	AVG-FID(f_j, X, h)	AVG-FID(f_j, g, h)	Feature f_j	$ g $	Defining Features
Student	LIME	-.006	-.011	Failures	.01	Alcohol Use, Urban Home
	SHAP	-.15	-2.1	Absences	.02	Parental Status, Urban Home
	LR	21.7	-4.0	Father WFH	.03	Alcohol Use, Health
COMPAS R	LIME	.0009	-.14	Age	.05	Native-American
	SHAP	.012	.41	Age	.04	Asian-American
	LR	.5	1.17	Native American	.04	Asian/Hispanic-American
COMPAS D	GRAD	.07	.16	Arrest, No Charge	.05	Asian/Native-American
	LIME	-.0003	-.06	Age	.02	Native/Black-American
	SHAP	.06	2.35	Age	.07	Black/Asian-American
Bank	LR	6.7	10.7	Caucasian	.04	Native-American
	LIME	-.003	.03	# of Employees	.03	Marital Status
	SHAP	-.004	.016	Euribor Rate	.03	Marital Status
Folktables	LR	-.07	-.0045	Illiterate	.01	Age, Marital Status
	LIME	-.0007	-.11	Age	.21	Marital Status
	SHAP	.023	.15	Education	.03	Asian-American
	LR	-.26	-.06	Self-Employed	.02	White-American

We defer the details in how we implemented Algorithm 1 and optimized Equation 5 to Appendix D.

5.2 Summary of Results

Table 2 summarizes all the experiments run, displaying the subgroup/feature pair with the highest FID for each dataset and importance notion. It also shows the size of the subgroup and the subgroup’s main defining features. This is further visualized in Figure 1. The values in Figure 1 are scaled as $|\log_{10}(R)|$ where R is the ratio of average feature importance between the subgroup and the whole dataset. As we can see, across each dataset and method, there exist subgroups with high FID, often differing by orders of magnitude. For example, on Folktables with LIME as the importance notion, there is a subgroup on which age is on average, 225 times more important than it is for the whole population.

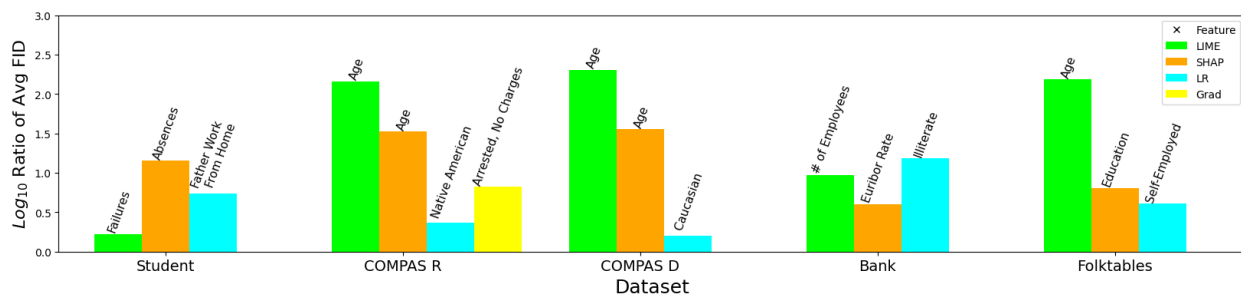


Figure 1: Summary of the highest FIDs found for each dataset and method. For cross-dataset comparison, this is displayed as $|\log_{10}(R)|$ where R is the ratio of average importance per data point for separable notions and the ratio of coefficients for the linear coefficient notion. The feature associated with each top subgroup is written above each bar.

A natural follow up question that arises from this experiment is what does the distribution of FIDs look like for a given dataset? Figure 2 shows a distribution of the 15 features on the Bank dataset with the highest FID values. As we can see, there are a few features where large FID subgroups can be found, but it tails off significantly after that. This pattern is replicated across all datasets and feature importance notions. This is a positive result, because it means that when auditing a dataset for fairness concerns using our method, an analyst or domain expert can focus on a handful of features that perform drastically differently on specific subgroups, since the majority of features do not behave significantly different on any sensitive subgroups.

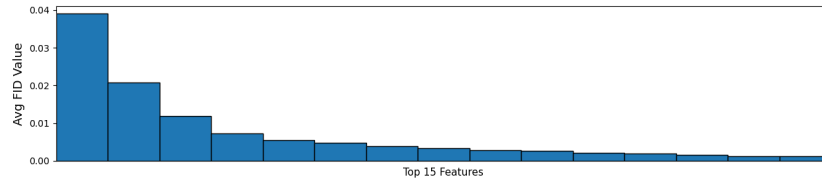


Figure 2: Distribution of FIDs on the top features from the BANK dataset using LIME importance notion. We can see a sharp drop off in FID for the features. This is replicated in all datasets and methods

5.3 Discussion of high AVG-FID subgroups

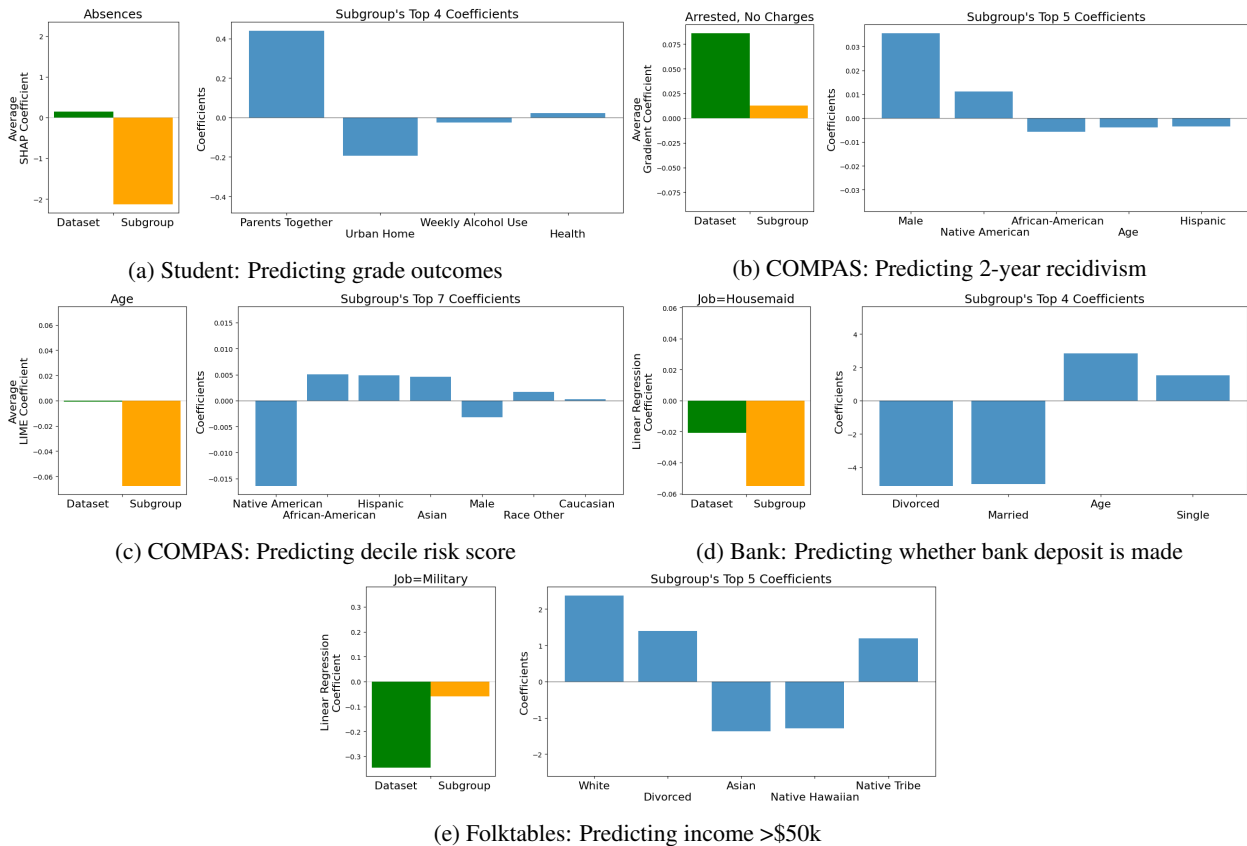


Figure 3: Exploration of key subgroup/feature pairs found for each dataset. The first graph shows the change in feature importance from whole dataset to subgroup. The second graph shows the main coefficients that define the subgroup.

In Figure 3, we highlight selections of an interesting (feature, subgroup, method) pair for each dataset. Figure 3a shows that on the Student dataset the feature absences which is of near zero importance on the dataset as a whole, is extremely negatively correlated with student performance on a subgroup whose top 2 features indicate whether a student’s parents are together, and if they live in a rural neighborhood. Figure 3b shows that on the COMPAS dataset with method GRAD, the feature arrested-but-with-no-charges is typically highly important when predicting

two-year-recidivism. However, it carries significantly less importance on a subgroup that is largely defined as Native American males. When predicting the decile risk score on COMPAS, LIME indicates that age is not important on the dataset as a whole; however, for non-Native American, female minorities, older age can be used to explain a lower Decile Score. On the Bank dataset using LIN-FID, we see that a linear regression trained on points from a subgroup defined by older, single individuals, puts more importance on `job=housemaid` when predicting likelihood in signing up for an account. Finally on Folktables, we see that LIN-FID assigns much lower weight to the `job=military` feature among a subgroup that is mainly white and divorced people than in the overall dataset when predicting income. These interesting examples, in conjunction with the results reported in Table 2, highlight the usefulness of our method in finding subgroups where a concerned analyst/domain expert could dig deeper to determine how biases might be manifesting themselves in the data and if/how to correct for them.

5.4 Statistical Validity of Results: Generalization of AVG-FID and $|g|$

When confirming the validity of our findings, there are two potential concerns:

1. Are the subgroup sizes found in-sample approximately the same on the test set?
2. Do the FID’s found on the training set generalize to the test set?

In Figure 4, we can see that when we take the maximal subgroup found for each feature f_j , g_j^* , and compute it’s size $|g_j^*|$ on the test set, for both the separable and non-separable methods it almost always fell within the specified $[\alpha_L, \alpha_U]$ range. Additionally, the average difference in size between the train and test subgroups was less than .005 on all notions of feature importance and all datasets except for Student, which tended to have differences closer to .025 due to its smaller size. A few rare subgroups were significantly outside the desired α range, which was typically due to the degenerate case of the feature importance values all being 0 for the feature in question. Additional subgroup size plots are provided in Appendix F.

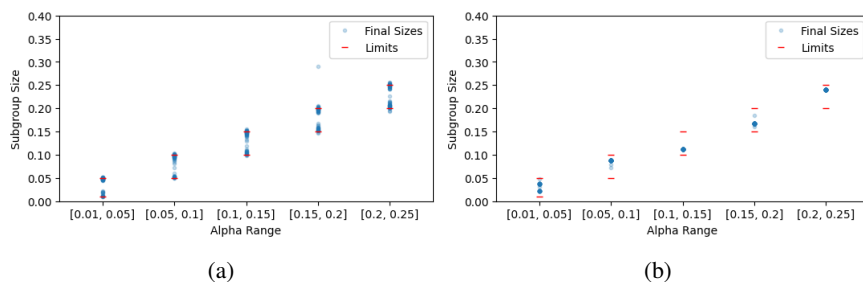


Figure 4: Final subgroup sizes compared with α ranges using Folktables dataset. (a) Outcome from the separable approach and (b) Outcome from the non-separable method. We see appropriate returns for all datasets and methods (see Appendix F for more)

Figure 5 compares the train and test values of $\text{AVG-FID}(g_j^*, j)$ for each feature f_j on the Folktables dataset for methods LIME, SHAP, and Linear Regression, and on the COMPAS R dataset for GRAD. The separable methods all generalized extremely well. Linear Regression still generalized, although not as robustly, with a few outlier values occurring. This was due to ill-conditioned design matrices for small subgroups leading to instability in fitting the least squares estimator. In Figure 10 in the Appendix, we investigate the difference between the feature importance computed on the whole training dataset, and on the whole test dataset. The results show that for Linear Regression in particular, for some features the importance on the train and test datasets differ significantly, indicating that the lack of generalization in Figure 5 is likely due to the feature importance method itself failing to generalize, rather than over-fitting via the selection of the maximal AVG-FID subgroup g_j^* .

Some testing was also done on the choice of hypothesis class h for the separable methods. For the LIME and SHAP notion on the COMPAS dataset, h was trained as both a Random Forest and Logistic Regression model and the outcomes of the algorithm were consistent with each other. Using either classifier, age and num-prior-crimes were found to be the two features with significant FID, the other features came in roughly similar order but with small enough FID values to be unimportant. Likewise, the subgroups with FID were defined similarly between the choices of h : for age, both subgroups were defined by young, non-asians, and for num-prior-crimes they were defined by non-Native American females.

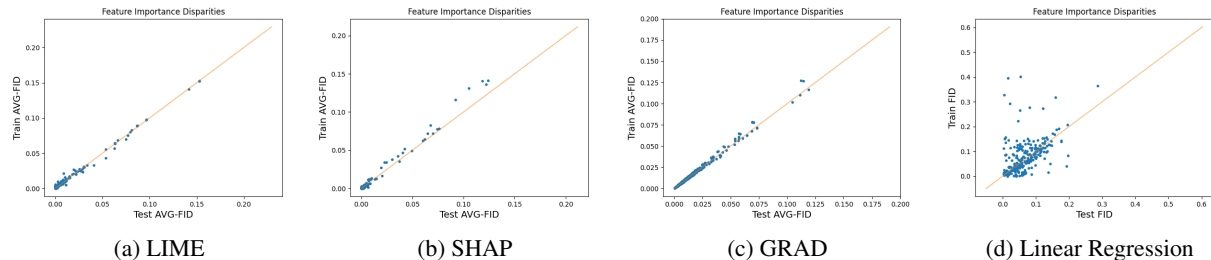


Figure 5: Generalizability of AVG-FID. Each dot represents a feature, the x-value is $\text{AVG-FID}(f_j, g(X_{test}))$, and y-value is $\text{AVG-FID}(f_j, g(X_{train}))$. (a), (b), and (d) are computed on the Folktables dataset and (c) is computed on the COMPAS R dataset. The closer the dots are to the diagonal line, the better the approach generalizes. The non-separable approach suffers slightly from the instability of the WLS method.

5.5 Comparison of AVG-FID values on rich vs. marginal subgroups

To better justify the use of rich subgroups, we performed the same analysis but only searching over the marginal subgroup space. For each dataset and importance notion pair, we established the finite list of marginal subgroups defined by a single sensitive characteristic and computed the feature importances on each of these subgroups. In Figure 6, we compare the maximal AVG-FID rich subgroups shown in Figure 1 to the maximal AVG-FID marginal subgroup for the same feature. In about half of the cases, the AVG-FID of the marginal subgroup was similar to the rich subgroup. In the other cases, expanding our subgroup classes to include rich subgroups defined by linear functions of the sensitive attributes enabled us to find a subgroup that had a significantly higher AVG-FID. The best example of this is on the Folktables dataset using the linear regression notion of importance (LR). We were able to find a rich subgroup where the feature `Self-Employed` had AVG-FID 4 times less than the AVG-FID on the full dataset. However, we were unable to find any subgroup in the marginal space where the importance of the feature `Self-Employed` was substantially different. In some cases in Figure 6, the marginal subgroup performs slightly better than the rich subgroup. This happens when using rich subgroups does not offer any substantial advantage over marginal subgroups, and the empirical error tolerance in Algorithm 1 stopped the convergence early.

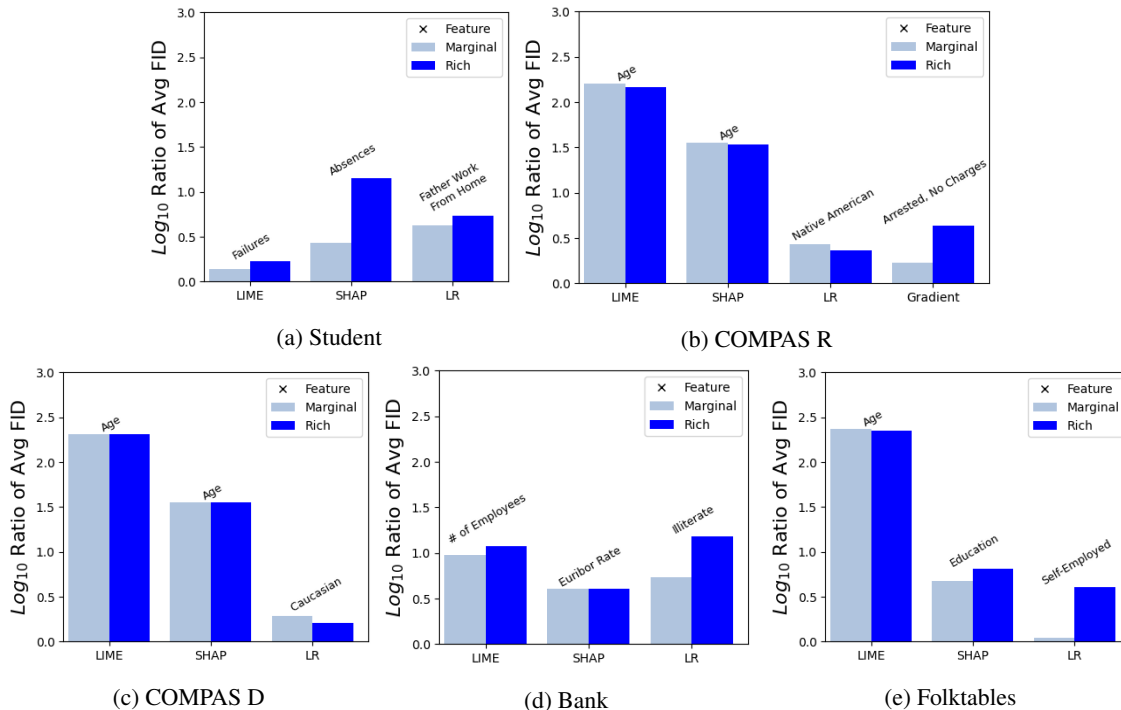


Figure 6: Comparison of the maximal FID rich subgroups from Figure 1 to the maximal FID marginal subgroup on the same feature. This is displayed as $|\log_{10}(R)|$ where R is the ratio of average importance per data point for separable notions and the ratio of coefficients for the linear coefficient notion. The feature associated with the subgroups is written above each bar.

6 Acknowledgements

The authors would like to thank Cynthia Dwork for the initial conversations that motivated the problem direction.

References

- [1] Michael J. Kearns, Seth Neel, Aaron Roth, and Zhiwei Steven Wu. Preventing fairness gerrymandering: Auditing and learning for subgroup fairness. *CoRR*, abs/1711.05144, 2017.
- [2] Úrsula Hébert-Johnson, Michael P. Kim, Omer Reingold, and Guy N. Rothblum. Calibration for the (computationally-identifiable) masses. *CoRR*, abs/1711.08513, 2017.
- [3] Julia Angwin, Jeff Larson, Surya Mattu, and Lauren Kirchner. Machine bias: There’s software used across the country to predict future criminals. and it’s biased against blacks., 2016. [accessed: 15.11.2020].
- [4] Xolani Dastile, Turgay Celik, and Moshe Potsane. Statistical and machine learning models in credit scoring: A systematic literature survey. *Applied Soft Computing*, 91:106263, 2020.
- [5] Emily Keddell. Algorithmic justice in child protection: Statistical fairness, social justice and the implications for practice. *Social Sciences*, 8(10), 2019.
- [6] Solon Barocas, Moritz Hardt, and Arvind Narayanan. *Fairness and Machine Learning: Limitations and Opportunities*. fairmlbook.org, 2019. <http://www.fairmlbook.org>.
- [7] Simon Caton and Christian Haas. Fairness in machine learning: A survey. *CoRR*, abs/2010.04053, 2020.
- [8] Tom B. Brown, Benjamin Mann, Nick Ryder, Melanie Subbiah, Jared Kaplan, Prafulla Dhariwal, Arvind Neelakantan, Pranav Shyam, Girish Sastry, Amanda Askell, Sandhini Agarwal, Ariel Herbert-Voss, Gretchen Krueger, Tom Henighan, Rewon Child, Aditya Ramesh, Daniel M. Ziegler, Jeffrey Wu, Clemens Winter, Christopher Hesse, Mark Chen, Eric Sigler, Mateusz Litwin, Scott Gray, Benjamin Chess, Jack Clark, Christopher Berner, Sam McCandlish, Alec Radford, Ilya Sutskever, and Dario Amodei. Language models are few-shot learners. *CoRR*, abs/2005.14165, 2020.

- [9] Alec Radford, Jong Wook Kim, Chris Hallacy, Aditya Ramesh, Gabriel Goh, Sandhini Agarwal, Girish Sastry, Amanda Askell, Pamela Mishkin, Jack Clark, Gretchen Krueger, and Ilya Sutskever. Learning transferable visual models from natural language supervision. *CoRR*, abs/2103.00020, 2021.
- [10] Nathaniel Swinger, Maria De-Arteaga, Neil Thomas Heffernan IV, Mark D. M. Leiserson, and Adam Tauman Kalai. What are the biases in my word embedding? *CoRR*, abs/1812.08769, 2018.
- [11] Paul Pu Liang, Chiyu Wu, Louis-Philippe Morency, and Ruslan Salakhutdinov. Towards understanding and mitigating social biases in language models. *CoRR*, abs/2106.13219, 2021.
- [12] Claire Miller. Algorithms and bias: Q. and a. with cynthia dwork, Aug 2015.
- [13] Marco Túlio Ribeiro, Sameer Singh, and Carlos Guestrin. "why should I trust you?": Explaining the predictions of any classifier. *CoRR*, abs/1602.04938, 2016.
- [14] Scott M. Lundberg and Su-In Lee. A unified approach to interpreting model predictions. *CoRR*, abs/1705.07874, 2017.
- [15] Karen Simonyan, Andrea Vedaldi, and Andrew Zisserman. Deep inside convolutional networks: Visualising image classification models and saliency maps. *CoRR*, abs/1312.6034, 2013.
- [16] Christoph Molnar. *Interpretable Machine Learning*. 2 edition, 2022.
- [17] Michael J. Kearns, Seth Neel, Aaron Roth, and Zhiwei Steven Wu. An empirical study of rich subgroup fairness for machine learning. *CoRR*, abs/1808.08166, 2018.
- [18] Alexandra Chouldechova. Fair prediction with disparate impact: A study of bias in recidivism prediction instruments, 2016.
- [19] Jon M. Kleinberg, Sendhil Mullainathan, and Manish Raghavan. Inherent trade-offs in the fair determination of risk scores. *CoRR*, abs/1609.05807, 2016.
- [20] Satyapriya Krishna, Tessa Han, Alex Gu, Javin Pombra, Shahin Jabbari, Steven Wu, and Himabindu Lakkaraju. The disagreement problem in explainable machine learning: A practitioner’s perspective. *CoRR*, abs/2202.01602, 2022.
- [21] Alekh Agarwal, Alina Beygelzimer, Miroslav Dudík, John Langford, and Hanna M. Wallach. A reductions approach to fair classification. *CoRR*, abs/1803.02453, 2018.
- [22] Diederik P. Kingma and Jimmy Ba. Adam: A method for stochastic optimization. In Yoshua Bengio and Yann LeCun, editors, *3rd International Conference on Learning Representations, ICLR 2015, San Diego, CA, USA, May 7-9, 2015, Conference Track Proceedings*, 2015.
- [23] Paula Cortez and Alice Silva. Using data mining to predict secondary school student performance. In *Proceedings of 5th Future Business Technology Conference*, pages 5–12, 2008.
- [24] Sérgio Moro, Paulo Cortez, and Paulo Rita. A data-driven approach to predict the success of bank telemarketing. *Decision Support Systems*, 62:22–31, 2014.
- [25] Frances Ding, Moritz Hardt, John Miller, and Ludwig Schmidt. Retiring adult: New datasets for fair machine learning. *CoRR*, abs/2108.04884, 2021.
- [26] Lunjia Hu, Inbal Livni-Navon, Omer Reingold, and Chutong Yang. Omnipredictors for constrained optimization, 2022.
- [27] Parikshit Gopalan, Adam Tauman Kalai, Omer Reingold, Vatsal Sharan, and Udi Wieder. Omnipredictors. *CoRR*, abs/2109.05389, 2021.
- [28] Christopher Jung, Changhwa Lee, Mallesh M. Pai, Aaron Roth, and Rakesh Vohra. Moment multicalibration for uncertainty estimation. *CoRR*, abs/2008.08037, 2020.
- [29] Cynthia Dwork, Moritz Hardt, Toniann Pitassi, Omer Reingold, and Richard Zemel. Fairness through awareness. *Proceedings of the 3rd Innovations in Theoretical Computer Science Conference on - ITCS '12*, 2012.
- [30] Matthew Joseph, Michael Kearns, Jamie Morgenstern, Seth Neel, and Aaron Roth. Meritocratic fairness for infinite and contextual bandits. In *Proceedings of the 2018 AAAI/ACM Conference on AI, Ethics, and Society, AIES '18*, page 158–163, New York, NY, USA, 2018. Association for Computing Machinery.
- [31] Moritz Hardt, Eric Price, and Nathan Srebro. Equality of opportunity in supervised learning. *CoRR*, abs/1610.02413, 2016.
- [32] Geoff Pleiss, Manish Raghavan, Felix Wu, Jon M. Kleinberg, and Kilian Q. Weinberger. On fairness and calibration. *CoRR*, abs/1709.02012, 2017.
- [33] Matt J. Kusner, Joshua R. Loftus, Chris Russell, and Ricardo Silva. Counterfactual fairness, 2017.

- [34] Faisal Kamiran and Toon Calders. Data preprocessing techniques for classification without discrimination. *Knowledge and information systems*, 33(1):1–33, 2012.
- [35] Tatiana Tommasi, Novi Patricia, Barbara Caputo, and Tinne Tuytelaars. A deeper look at dataset bias. In *Domain adaptation in computer vision applications*, pages 37–55. Springer, 2017.
- [36] Yi Li and Nuno Vasconcelos. Repair: Removing representation bias by dataset resampling. In *2019 IEEE/CVF Conference on Computer Vision and Pattern Recognition (CVPR)*, pages 9564–9573, 2019.
- [37] Mukund Sundararajan, Ankur Taly, and Qiqi Yan. Axiomatic attribution for deep networks. *CoRR*, abs/1703.01365, 2017.
- [38] David Baehrens, Timon Schroeter, Stefan Harmeling, Motoaki Kawanabe, Katja Hansen, and Klaus-Robert Mueller. How to explain individual classification decisions, 2009.
- [39] J. R. Quinlan. Induction of decision trees. *Machine Learning*, 1(1):81–106, 1986.
- [40] Jiachang Liu, Chudi Zhong, Margo Seltzer, and Cynthia Rudin. Fast sparse classification for generalized linear and additive models, 2022.
- [41] Przemyslaw A. Grabowicz, Nicholas Perello, and Aarshee Mishra. Marrying fairness and explainability in supervised learning. In *2022 ACM Conference on Fairness, Accountability, and Transparency*. ACM, jun 2022.
- [42] Tom Begley, Tobias Schwedes, Christopher Frye, and Ilya Feige. Explainability for fair machine learning. *CoRR*, abs/2010.07389, 2020.
- [43] Eric Ingram, Furkan Gursoy, and Ioannis A. Kakadiaris. Accuracy, fairness, and interpretability of machine learning criminal recidivism models, 2022.
- [44] Jürgen Kindler. A simple proof of sion’s minimax theorem. *Am. Math. Mon.*, 112(4):356–358, 2005.
- [45] Yoav Freund and Robert E. Schapire. Game theory, on-line prediction and boosting. In *Proceedings of the Ninth Annual Conference on Computational Learning Theory*, COLT ’96, page 325–332, New York, NY, USA, 1996. Association for Computing Machinery.
- [46] Jyrki Kivinen and Manfred K. Warmuth. Exponentiated gradient versus gradient descent for linear predictors. *Inf. Comput.*, 132(1):1–63, 1997.
- [47] Chirag Agarwal, Satyapriya Krishna, Eshika Saxena, Martin Pawelczyk, Nari Johnson, Isha Puri, Marinka Zitnik, and Himabindu Lakkaraju. Openxai: Towards a transparent evaluation of model explanations, 2022.
- [48] US Census Bureau. 2014-2018 acs pums data dictionary, 2020.

A Proof of Theorem 1

Theorem 1: Let F a separable FID, fix a classifier h , subgroup class \mathcal{G} , and oracle $\text{CSC}_{\mathcal{G}}$. Then fixing a feature of interest f_j , we will run Algorithm 1 twice; once with FID given by F , and once with FID given by $-F$. Let $\hat{p}_{\mathcal{G}}^T$ be the distribution returned after $T = O(\frac{4n^2 B^2}{\nu^2})$ iterations by Algorithm 1 that achieves the larger value of $\mathbb{E}[\text{FID}(g, j)]$. Then:

$$\begin{aligned} \text{FID}(g_j^*, j) - \mathbb{E}_{g \sim \hat{p}_{\mathcal{G}}^T}[\text{FID}(g, j)] &\leq \nu \\ |\Phi_L(g)|, |\Phi_U(g)| &\leq \frac{1 + 2\nu}{B} \end{aligned} \quad (6)$$

Proof. We start by transforming our constrained optimization into optimizing a min – max objective. The min player, referred to as the *subgroup player* will be solving a CSC problem over the class \mathcal{G} at each iteration, while the max player, called the *dual player*, will be adjusting the dual weights λ on the two constraints using the exponentiated gradient algorithm [46]. By Lemma 2 [45], we know that if each player implements a *no-regret* strategy, then the error of subgroup found after T rounds is sub-optimal by at most the average cumulative regret of both players. The regret bound for the exponentiated gradient descent ensures this occurs in *poly*(n) rounds.

As in [1, 21], we first relax Equation 2 to optimize over all *distributions* over subgroups, and we enforce that our constraints hold in expectation over this distribution. Our new optimization problem becomes:

$$\begin{aligned} \min_{p_g \in \Delta(\mathcal{G})} \quad & \mathbb{E}_{g \sim p_g} \left[\sum_{i=1}^n g(x_i) F'(f_j, x_i, h) \right] \\ \text{s.t.} \quad & \mathbb{E}_{g \sim p_g} [\Phi_L(g)] \leq 0 \\ & \mathbb{E}_{g \sim p_g} [\Phi_U(g)] \leq 0 \end{aligned} \quad (7)$$

We note that while $|\mathcal{G}|$ may be infinite, the number of distinct labelings of X by elements of \mathcal{G} is finite; we denote the number of these by $|\mathcal{G}(X)|$. Then since Equation 7 is a finite linear program in $|\mathcal{G}(X)|$ variables, it satisfies strong duality, and we can write:

$$\begin{aligned} (p_g^*, \lambda^*) &= \text{argmin}_{p_g \in \Delta(\mathcal{G})} \text{argmax}_{\lambda \in \Lambda} \mathbb{E}_{g \sim p_g} [L(g, \lambda)] = \text{argmin}_{p_g \in \Delta(\mathcal{G})} \text{argmax}_{\lambda \in \Lambda} L(p_g, \lambda) \\ \text{with } L(g, \lambda) &= \sum_{x \in X} g(x) F(f_j, x, h) + \lambda_L \Phi_L + \lambda_U \Phi_U, \quad L(p_g, \lambda) = \mathbb{E}_{g \sim p_g} [L(g, \lambda)] \end{aligned}$$

As in [1] $\Lambda = \{\lambda \in \mathbb{R}^2 \mid \|\lambda\|_1 \leq B\}$ is chosen to make the domain compact, and does not change the optimal parameters as long as B is sufficiently large, e.g. $\|\lambda^*\|_1 \leq B$. In practice, this is a hyperparameter of Algorithm 1, similar to [21, 1]. Then we follow the development in [21, 1] to show that we can compute (p_g^*, λ^*) efficiently by implementing *no-regret* strategies for the subgroup player (p_g) and the dual player (λ).

Formally, since $\mathbb{E}_{g \sim p_g} [L(g, \lambda)]$ is bi-linear in p_g, λ , and $\Lambda, \Delta(\mathcal{G})$ are convex and compact, by Sion's minimax theorem [44]:

$$\min_{p_g \in \Delta(\mathcal{G})} \max_{\lambda \in \Lambda} L(p_g, \lambda) = \max_{\lambda \in \Lambda} \min_{p_g \in \Delta(\mathcal{G})} L(p_g, \lambda) = \text{OPT} \quad (8)$$

Then by Theorem 4.5 in [1], we know that if (p_g^*, λ^*) is a ν -approximate min-max solution to Equation 8 in the sense that

$$\begin{aligned} \text{if: } L(p_g^*, \lambda^*) &\leq \min_{p \in \Delta(\mathcal{G})} L(p, \lambda^*) + \nu, \quad L(p_g, \lambda) \geq \max_{\lambda \in \Lambda} L(p^*, \lambda), \\ \text{then: } F(f_j, p_g^*, h) &\leq \text{OPT} + 2\nu, \quad |\Phi_L(g)|, |\Phi_U(g)| \leq \frac{1 + 2\nu}{B} \end{aligned} \quad (9)$$

So in order to compute an approximately optimal subgroup distribution p_g^* , it suffices to compute an approximate min-max solution of Equation 8. In order to do that we rely on the classic result of [45] that states that if the subgroup player best responds, and if the dual player achieves low regret, then as the average regret converges to zero, so does the sub-optimality of the average strategies found so far.

Lemma 2 ([45]). *Let $p_1^\lambda, \dots, p_T^\lambda$ be a sequence of distributions over Λ , played by the dual player; and let g^1, \dots, g^T be the subgroup players best responses against these distributions respectively. Let $\hat{\lambda}_T = \frac{1}{T} \sum_{t=1}^T p_t^\lambda$, $\hat{p}_g = \frac{1}{T} \sum_{t=1}^T g_t$. Then if*

$$\sum_{t=1}^T \mathbb{E}_{\lambda \sim p_t^\lambda} [L(g_t, \lambda)] - \min_{\lambda \in \Lambda} \sum_{t=1}^T [L(g_t, \lambda)] \leq \nu T,$$

Then $(\hat{\lambda}_T, \hat{p}_g)$ is a ν -approximate minimax equilibrium of the game.

To establish Theorem 1, we need to show (i) that we can efficiently implement the subgroup players best response using $\text{CSC}_{\mathcal{G}}$ and (ii) we need to translate the regret bound for the dual players best response into a statement about optimality, using Lemma 2. Establishing (i) is immediate, since at each round t , if $\lambda_{t,0} = \mathbb{E}_{p_t^\lambda}[\lambda_L]$, $\lambda_{t,1} = \mathbb{E}_{p_t^\lambda}[\lambda_U]$, then the best response problem is:

$$\operatorname{argmin}_{p_g \in \Delta(G)} \mathbb{E}_{g \sim p_g} \left[\sum_{x \in X} g(x) F(f_j, x, h) + \lambda_{t,0} \Phi_L + \lambda_{t,1} \Phi_U \right]$$

Which can further be simplified to:

$$\operatorname{argmin}_{g \in G} \sum_{x \in X} g(x) (F(f_j, x, h) - \lambda_L + \lambda_U) \quad (10)$$

This can be computed with a single call of $\text{CSC}_{\mathcal{G}}$, as desired. To establish (ii), the no-regret algorithm for the dual player's distributions, we note that at each round the dual player is playing online linear optimization over 2 dimensions. Algorithm 1 implements the exponentiated gradient algorithm [46], which has the following guarantee proven in Theorem 1 of [21], which follows easily from the regret bound of exponentiated gradient [46], and Lemma 2:

Lemma 3 ([21]). *Setting $\eta = \frac{\nu}{2n^2B}$, Algorithm 1 returns \hat{p}_λ^T that is a ν -approximate min-max point in at most $O(\frac{4n^2B^2}{\nu^2})$ iterations.*

Combining this result with Equation 8 completes the proof. □

B F_{lin} Convexity Lemma

Lemma 4. F_{lin} as defined in Equation 4 is nonconvex.

Proof. We will prove this by contradiction. Assume F_{lin} is convex, which means the Hessian is positive semidefinite everywhere. First we will fix $(Xg(X)X^T)^{-1}$ to be the identity matrix, which we can do without loss of generality by scaling g by a constant. This scaling will not affect the convexity of F_{lin} .

Now, we have the simpler form of $F_{lin} = (X^T g(X) Y) \cdot e_j$. We then can compute the values of the Hessian:

$$\frac{\partial^2 F^2}{\partial^2 g} = (X^T g''(X) Y) \cdot e_j$$

Consider the case where X^T is a 2×2 matrix with rows 1, 0 and 0, -1 and Y is a vector of ones. If g weights the second column (i.e. feature) greater than the first, then the output Hessian will be positive semidefinite. But if g weights the first column greater than the first, then it will be negative semi-definite. Since the Hessian is not positive semidefinite everywhere, F_{lin} must be nonconvex over the space of g . □

C NP-Completeness

We will show below that the fully general version of this problem (allowing any poly-time F) is NP complete. First, we will define a decision variant of the problem:

$$\delta_{X,F,h,A} = \max_{g \in \mathcal{G}, f_j} (|F(f_j, g, h) - F(f_j, X, h)|) \geq A$$

Note that a solution to the original problem trivially solves the decision variant. First, we will show the decision variant is in NP, then we will show it is NP hard via reduction to the max-cut problem.

Lemma 5. *The decision version of this problem is in NP.*

Proof. Our witness will be the subset g and feature f_j such that

$$(|F(f_j, g, h) - F(f_j, X, h)|) \geq A$$

Given these 2, evaluation of the absolute value is polytime given that F is polytime, so the solution can be verified in polytime. \square

Lemma 6. *The decision version of this problem is NP hard.*

Proof. We will define our variables to reduce our problem to maxcut(Q, k). Given a graph defined with V, E as the vertex and edge sets of Q (with edges defined as pairs of vertices), we will define our F, X, G, A , and h as follows:

$$\begin{aligned} X &= V \\ h &= \text{constant classifier, maps every value to 1} \\ \mathcal{G} &= \mathcal{P}(V) \text{ i.e. all possible subsets of vertices} \\ F(j, g, h) &= |x \in E : x[0] \in g, x[1] \in g^c| \\ &\quad \text{-i.e. } F(j, g, h) \text{ returns the number of} \\ &\quad \text{edges cut by a particular subset, ignoring} \\ &\quad \text{its first and third argument.} \\ &\quad \text{(this is trivially computable in polynomial} \\ &\quad \text{time by iterating over the set of edges).} \\ A &= k \end{aligned}$$

Note that $F(j, X, h) = 0$ by definition, and that $F \geq 0$. Therefore, $|F(j, g, h) - F(j, X, h)| = F(j, g, h)$, and we see that $(|F(f_j, g, h) - F(f_j, X, h)|) \geq A$ if and only if g is a subset on Q that cuts at least $A = k$ edges. Therefore an algorithm solving the decision variant of the feature importance problem also solves maxcut. \square

D Experimental Details

Algorithmic Details: Separable Case. In order to implement Algorithm 1 over a range of $[\alpha_L, \alpha_U]$ values, we need to specify our dual norm B , learning rate η , number of iterations used T , rich subgroup class \mathcal{G} , and the associated oracle $\text{CSC}_{\mathcal{G}}$. We note that for each feature f_j , Algorithm 1 is run twice; one corresponding to maximizing $\text{FID}(f_j, g, h)$ and the other to minimizing. Note that in both cases our problem is a minimization, but when maximizing we simply negate all of the point wise feature importance values $F(f_j, x_i, h) \rightarrow -F(f_j, x_i, h)$. In all experiments our subgroup class \mathcal{G} consists of linear threshold functions over the sensitive features: $\mathcal{G} = \{\theta \in \mathbb{R}^{d_{sens}} : \theta((x, x')) = \mathbf{1}\{\theta'x > 0\}\}$. We implement $\text{CSC}_{\mathcal{G}}$ as in [21, 1] via linear regression, see Algorithm 2 in Appendix E. To ensure the dual player's response is strong enough to enforce desired size constraints, we empirically found that setting the hyperparameter $B = 10^4 \cdot \mu(f_j)$ works well, where $\mu(f_j)$ is the average absolute importance value for feature j over S , $\text{AVG-FID}(j, S)$. We set the learning rate for exponentiated gradient descent to $\eta = 10^{-5}$. Empirical testing showed that $\eta \cdot B$ should be on the order of $\mu(f_j)$ or smaller to ensure proper convergence. For all datasets and methods we ran for at most $T = 5000$ iterations, which we observe empirically was large enough for FID values to stabilize and for $\frac{1}{T} \sum_{t=1}^T |g_t| \in [\alpha_U, \alpha_L]$, with the method typically converging in $T = 3000$ iterations or less. See Appendix G for a sample of convergence plots.

Algorithmic Details: LIN-FID. For the non-separable approach, datasets were once again split into train and test sets. For Student, it was split 50-50, while Compas, Bank, and Folktables were split 80-20 train/test. The 50-50 split for Student was chosen so that a linear regression model would be properly fit on a small $g(X_{test})$. The parameter vector θ for a logistic regression classifier was randomly initialized with a PyTorch random seed of 0. We used an ADAM [22] optimizer with a learning rate of .05 as our heuristic solver for the loss function.

To enforce subgroup size constraints, $\lambda_s P_{size}$ must be on a significantly larger order than $\lambda_c F_{lin}(g, j)$. Empirical testing found that values of $\lambda_s = 10^5$ and $\lambda_c = 10^{-1}$ returned appropriate subgroup sizes and also ensured smooth convergence. The optimizer ran until it converged upon a minimized linear regression coefficient, subject to the size constraints. Experimentally, this took at most 1000 iterations, see Appendix H for a sample of convergence plots. After

solving twice for the minimum and maximum $F_{lin}(g, j)$ values and our subgroup function g is chosen, we solve the WLS problem on both X_{test} and $g(X_{test})$ to get the final FID.

FID Notions.

LIME: A random forest model h was trained on dataset X^n . Then each data point along with the corresponding probability outputs from the classifier were input into the LIME Tabular Explainer Python module. This returned the corresponding LIME explanation values. **SHAP:** This was done with the same method as LIME, except using the SHAP Explainer Python module. **Vanilla Gradient:** Labeled as *GRAD* in charts, the vanilla gradient importance notion was computed using the Gradient method from the OpenXAI library [47]. This notion only works on differentiable classifiers so in this case, h is a logistic regression classifier. We found there was no substantial difference between the choice of random forest or logistic regression for h when tested on other importance notions (see Section 5.4). Due to constraints on computation time, this method was only tested on the COMPAS dataset (using *Two Year Recidivism* as the target variable). **Linear Regression:** For the linear regression notion, the subgroup g was chosen to be in the logistic regression hypothesis class. For a given subgroup $g(X)$, the weighted least squares (WLS) solution is found whose linear coefficients θ_g then define the feature importance value $e_j \cdot \theta_g$. For details on the generalizability of these importance notions, see Appendix I.

Datasets:

Student: This dataset aims to predict student performance in a Portugese grade school using demographic and familial data. For the purposes of this experiment, the target variable was math grades at the end of the academic year. Student was by far the smallest of the four datasets at only 395 data points. The sensitive features in Student are gender, parental status, address (urban or rural), daily alcohol consumption, weekly alcohol consumption, and health. Age typically would be considered sensitive but since in the context of school, age is primarily an indicator of class year, this was not included as a sensitive feature. The categorical features address, Mother’s Job, Father’s Job, and Legal Guardian were one hot encoded.

COMPAS: This dataset uses a pre-trial defendant’s personal background and past criminal record to predict risk of committing new crimes. To improve generalizability, we removed any criminal charge features that appeared fewer than 10 times. Binary counting features (e.g. 25-45 yrs old or 5+ misdemeanors) were dropped in favor of using the continuous feature equivalents. Additionally, the categorical variable Race was one-hot encoded. This brought the total number of features to 95. The sensitive features in COMPAS are age, gender, and race (Caucasian, African-American, Asian, Hispanic, Native American, and Other). For COMPAS, we ran all methodologies twice, once using the binary variable, *Two Year Recidivism*, as the target variable and once using the continuous variable *Decile Score*. *Two Year Recidivism* is what the model is intended to predict and is labeled as *COMPAS R* in the following sections. Meanwhile, *Decile Score* is what the COMPAS system uses in practice to make recommendations to judges and is labeled as *COMPAS D* in the following sections.

Bank: This dataset looks at whether a potential client signed up for a bank account after being contacted by marketing personnel. The sensitive features in Bank are age and marital status (married, single, or divorced). The age feature in Bank is a binary variable representing whether the individual is above the age of 25.

Folktables: This dataset is derived from US Census Data. Folktables covers a variety of tasks, but we used the ACSIncome task, which predicts whether an individual makes more than \$50k per year. The ACSIncome task is meant to mirror the popular Adult dataset, but with modifications to address sampling issues. For this paper, we used data from the state of Michigan in 2018. In order to reduce sparseness of the dataset, the Place of Birth feature was dropped for being extremely sparse and the Occupation features were consolidated into categories of work as specified in the official Census dictionary [48], (e.g. people who work for the US Army, Air Force, Navy, etc. were all consolidated into Occupation=Military). The sensitive features in Folktables are age, sex, marital status (married, widowed, divorced, separated, never married/under 15 yrs old), and race (Caucasian, African-American, Asian, Native Hawaiian, Native American singular tribe, Native American general, Other, and 2+ races).

E Cost Sensitive Classifier, CSC_G

Algorithm 2 CSC_G

Input: Dataset $X \subset \mathbb{R}^{d_{sens}} \times \mathbb{R}^{d_{safe}}$, costs $(c^0, c^1) \in \mathbb{R}^n$
 Let X_{sens} consist of the sensitive attributes x of each $(x, x') \in X$.
 Train linear regressor $r_0 : \mathbb{R}^{d_{sens}} \rightarrow \mathbb{R}$ on dataset (X_{sens}, c^0) ▷ learn to predict the cost c^0
 Train linear regressor $r_1 : \mathbb{R}^{d_{sens}} \rightarrow \mathbb{R}$ on dataset (X_{sens}, c^1) ▷ learn to predict the cost c^1
 Define $g((x, x')) := \mathbf{1}\{(r_0 - r_1)(x) > 0\}$ ▷ predict 0 if the estimated $c_0 < c_1$
 Return g

F Subgroup Sizes Outcomes

Here we chart the subgroup sizes outputted by the algorithms across all dataset and importance notion combinations. As a whole, the final subgroup sizes were generally within the specified α range. Occasionally, there were subgroups which were significantly outside the expected range. Usually this was due to a large number of $F(f_j, g, h)$ being zero for a given feature.

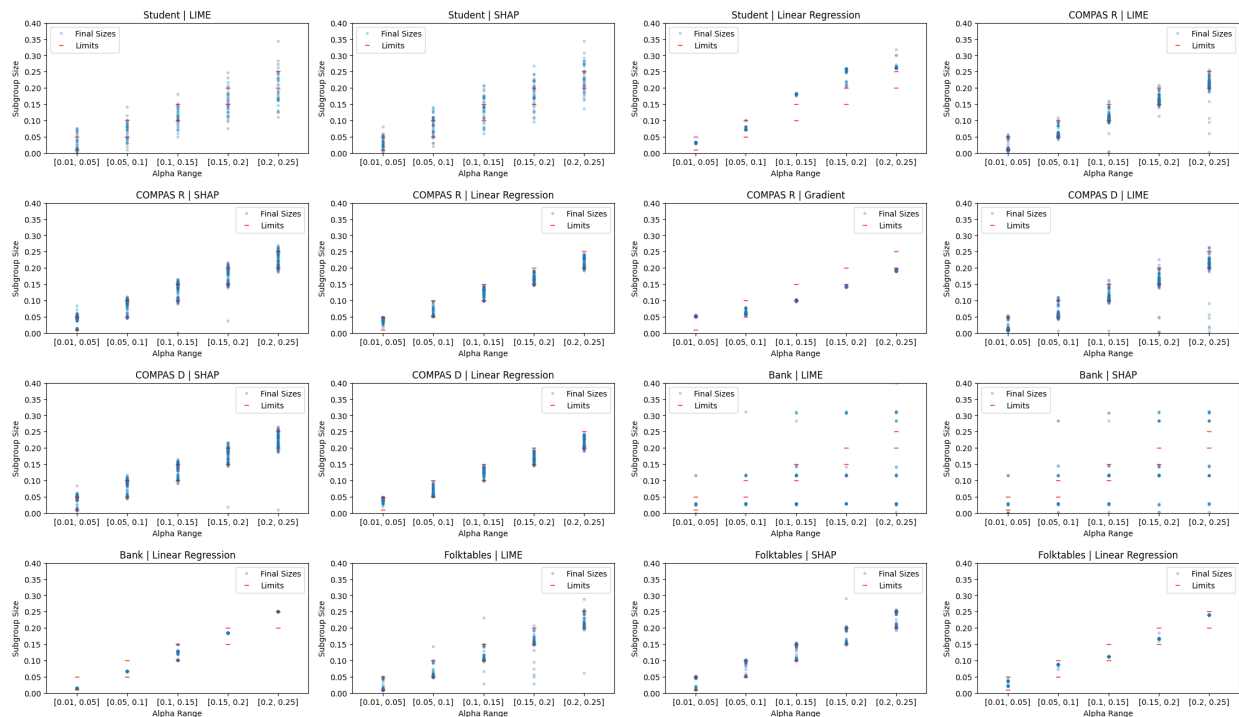


Figure 7: Final subgroup sizes compared with α ranges.

G Algorithm 1 Optimization Convergence

Here are additional graphs showing examples of the convergence of Algorithm 1. Data was tracked every 10 iterations, recording the Lagrangian values (to compute the error $v_t = \max(|L(\hat{p}_G^t, \hat{p}_\lambda^t) - \underline{L}|, |\bar{L} - L(\hat{p}_G^t, \hat{p}_\lambda^t)|)$), the subgroup size, and AVG-FID value, graphed respectively in Figure 8. We can see AVG-FID value moving upward, except when the subgroup size is outside the α range, and the Lagrangian error converging upon the set error bound v before terminating.

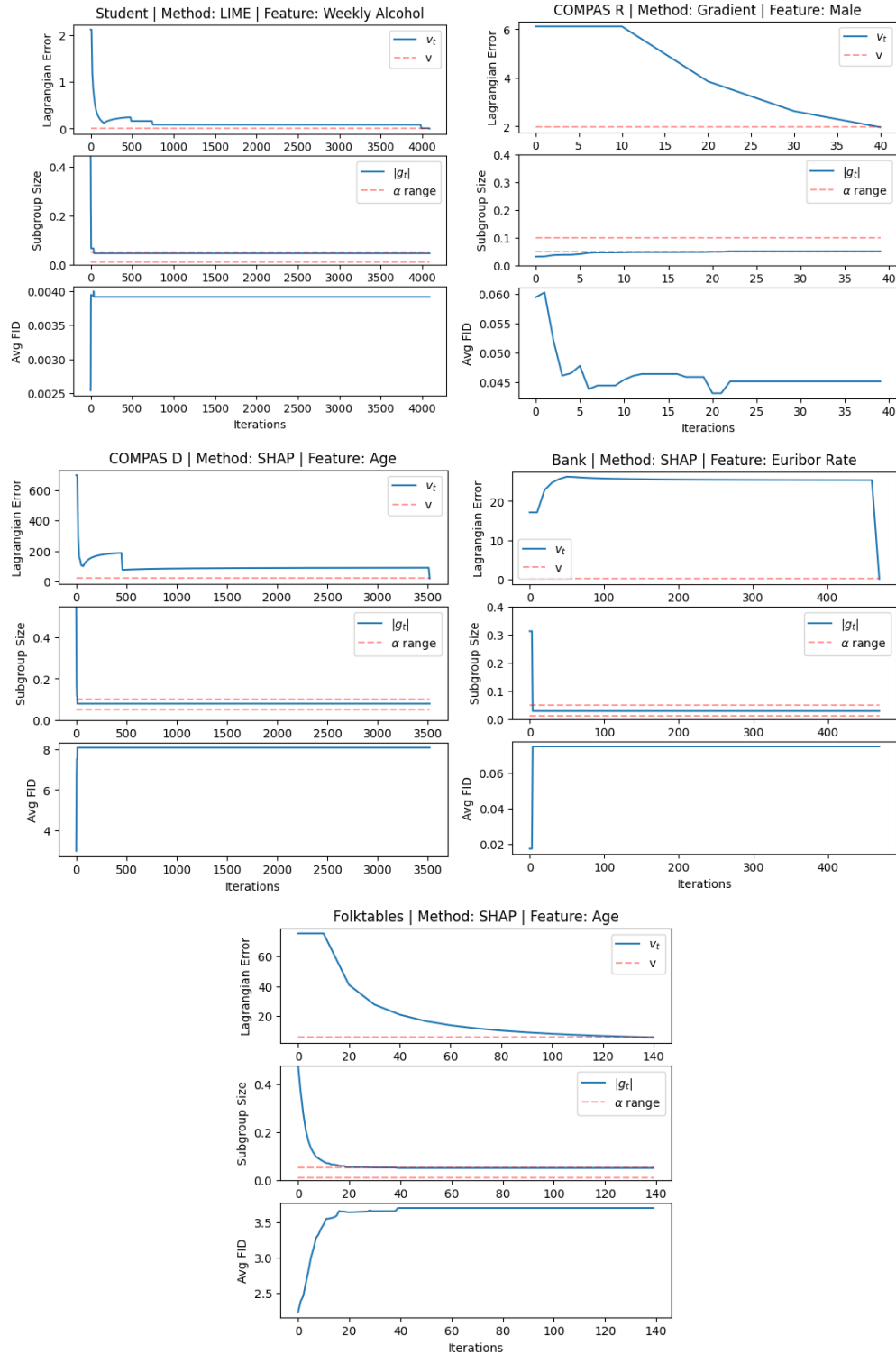


Figure 8: Plots detailing the convergence of Algorithm 1. The top plot shows the error convergence, i.e. the max difference in Lagrangian values between our solution and the min/max-players’ solution. The other two plots display the subgroup size and AVG-FID of the solution.

H Non-Separable Optimization Convergence

Here are additional graphs showing the convergence in the non-separable approach. Using the loss function that rewards minimizing the linear regression coefficient (or maximizing it) and having a size within the alpha constraints, we typically reach convergence after a few hundred iterations. In Figure 9, we can see in the respective upper graphs that the subgroup size rapidly goes to the α range and stays there. Meanwhile, the feature importance value oscillates rapidly as it tries to find the minimum/maximum value subject to the size constraints.

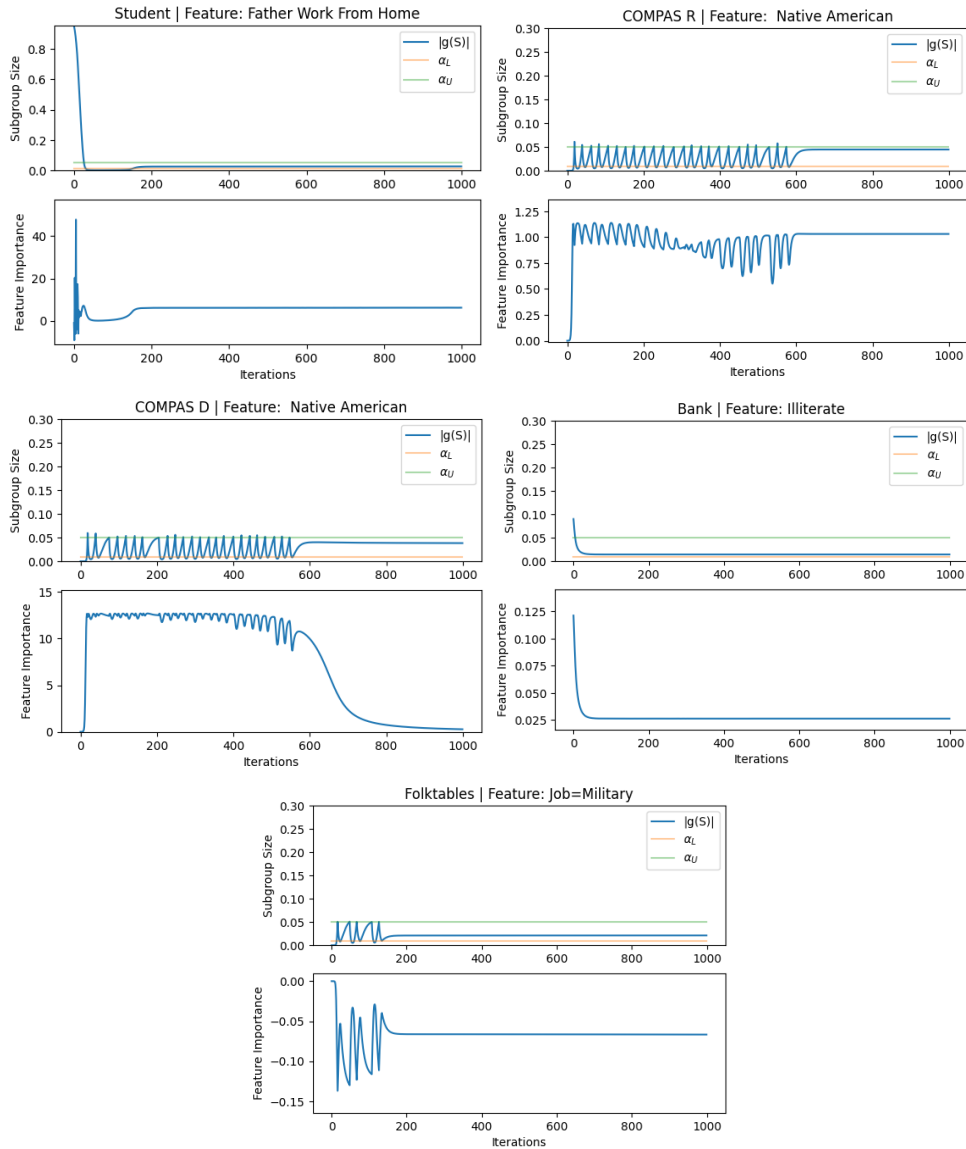


Figure 9: Plots of subgroup size and linear regression coefficient over the training iterations of the Adam optimizer. For each dataset, the feature with the highest FID was displayed.

I Importance Notion Generalization

To see if the different importance notions generalize out of sample, we plot the values of $F(f_j, X_{test}, h)$ against $F(f_j, X_{train}, h)$ with each point representing a feature f_j . The closer these points track the diagonal line, the better the importance notion generalizes. As we can see in Figure 10, LIME and GRAD generalize extremely well, with SHAP overfitting slightly. LIN-FID also generalizes less consistently, due to instability in fitting the least squares estimator on ill-conditioned design matrices.

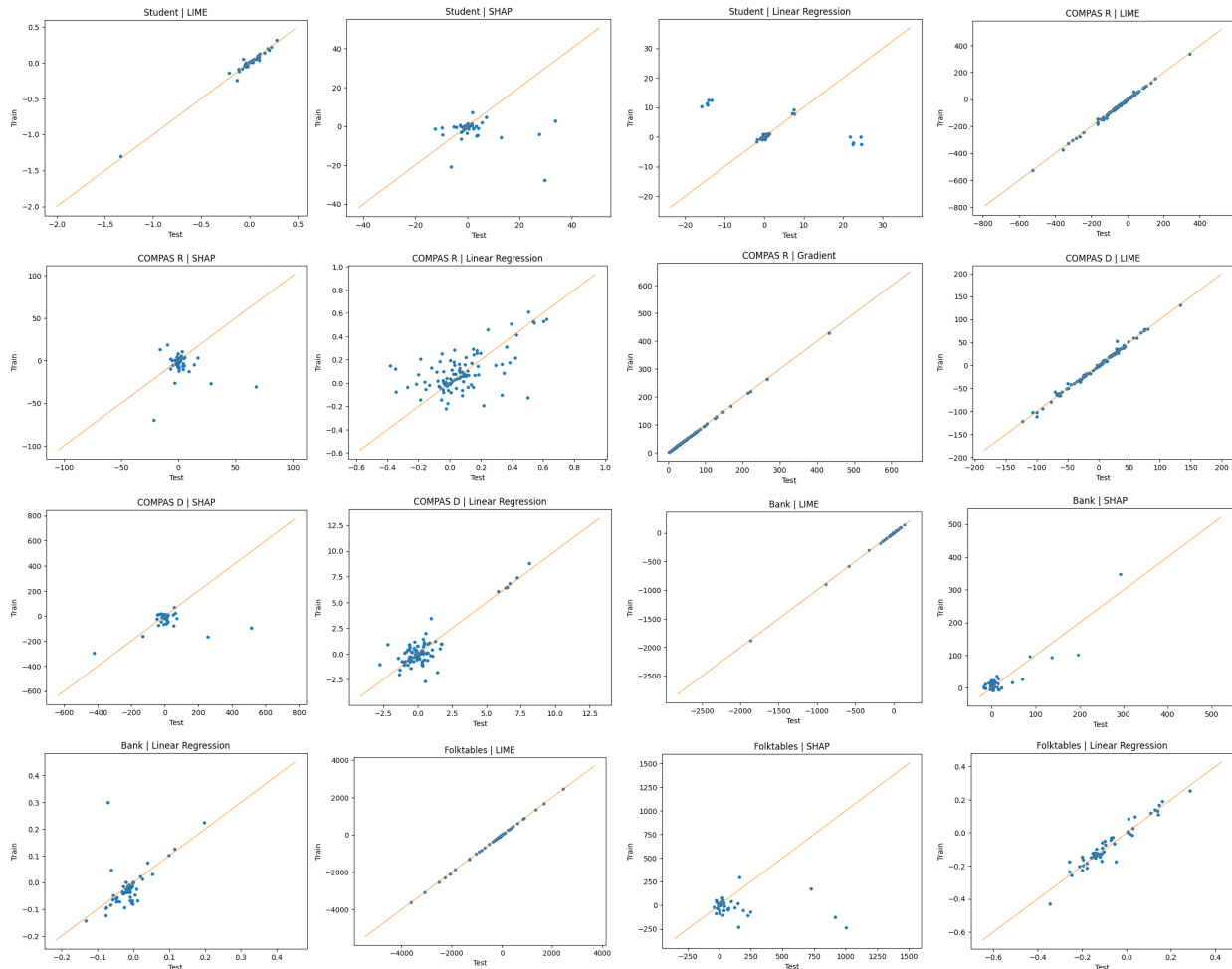


Figure 10: Generalization of importance notions. Each point represents a feature, the x-value is $F(f_j, X_{test})$, and y-value is $F(f_j, X_{train})$. The closer the points are to the diagonal, the more the notion generalizes.

J Ethical Review

There were no substantial ethical issues that came up during this research process. The datasets used are all publicly available, de-identified, and have frequently been used in fair machine learning research. There was no component of this research that sought to re-identify the data or use it in any fashion other than to test our methodology.